

Attenuation of low-frequency sound in the Northeast Pacific Ocean

R. K. Chow and R. G. Turner

Defense Research Establishment Pacific, Forces Mail Office, Victoria, British Columbia VOS 1B0, Canada

(Received 31 March 1982; accepted for publication 26 May 1982)

Long-range propagation losses were measured at frequencies from 0.025 to 0.8 kHz to the north and south of a receiver at 46°N, 143°30'W in the Northeast Pacific. To the south of the station, the attenuation losses experienced a pronounced minimum near 50 Hz and approached the one-half Thorp value at 0.8 kHz. An examination of the behavior of the attenuation coefficient as a function of range indicated that a range of at least 700 km would be required to make meaningful measurements of attenuation in this area. To the north of the receiving station, focusing of the sound due to a rapidly shallowing sound channel prevented reliable measurement of the attenuation coefficient at any range.

PACS numbers: 43.30.Bp, 92.10.Vz, 93.30.Pm

INTRODUCTION

As a result of extensive measurements carried out in the North Atlantic in the early 1950's, Marsh and Schulkin concluded that relaxation effects of magnesium sulfate ions were the dominant cause of the attenuation of sound in the ocean volume.¹ Some years later, Thorp^{2,3} examined additional data for the North Atlantic and Mediterranean and found that, although the magnesium sulfate ion explanation was appropriate for frequencies above 10 kHz, at lower frequencies a second relaxation mechanism was required to account for the anomalously high values observed. In 1973, Yeager *et al.*⁴ suggested that boric acid relaxation was probably the mechanism responsible. Recent measurements of attenuation, carried out in a number of oceans, tend to confirm that boric acid relaxation could account for most observed values of attenuation at frequencies between 0.2 and 10 kHz, although different concentrations of boric acid would be required for different ocean areas.⁵ At still lower frequencies, attenuation is too high for this explanation to apply and additional mechanisms such as sound scattering from inhomogeneities in the ocean volume have been invoked.⁵ Recently, Kibblewhite and his associates^{6,7} have concluded that, although attenuation losses below 200 Hz are generally independent of frequency, in some areas there is a distinct minimum near 50 Hz. A number of the above conclusions about the attenuation of sound below 1 kHz have been based, in part, on unpublished data provided by DREP. These data are presented in this letter along with details of the experimental and analysis procedures used.

I. EXPERIMENT AND ANALYSIS

In September 1973, a major experiment involving DREP and a number of U.S. defense laboratories was carried out to study acoustic environmental parameters in the Northeast Pacific. The primary DREP responsibilities were the collection of oceanographic data in the Gulf of Alaska and the measurement of sound propagation and ambient noise at the location shown in Fig. 1 (46°00'N, 143°30'W). The sound propagation experiment was conducted along the 143°30'W meridian both to the north and south of the receiver. To the south, SUS charges were dropped at approximately 1.85-km intervals by a ship which started at 28°30'N and

traveled north towards the receiver. To the north, SUS charges were dropped from an aircraft at approximately 15-km intervals along a track extending from the receiver to the Alaskan Shelf. Thus ranges in excess of 1000 km were realized both to the north and south of the receiver.

The experiment covered different oceanic zones with Eastern North Pacific water in the south and subarctic Pacific water in the north. A transition zone separating the two water masses extended roughly from 42°30'N to 47°30'N.

The bathymetry and sound-speed profiles along the track are shown in Fig. 2. Along the southern segment of the

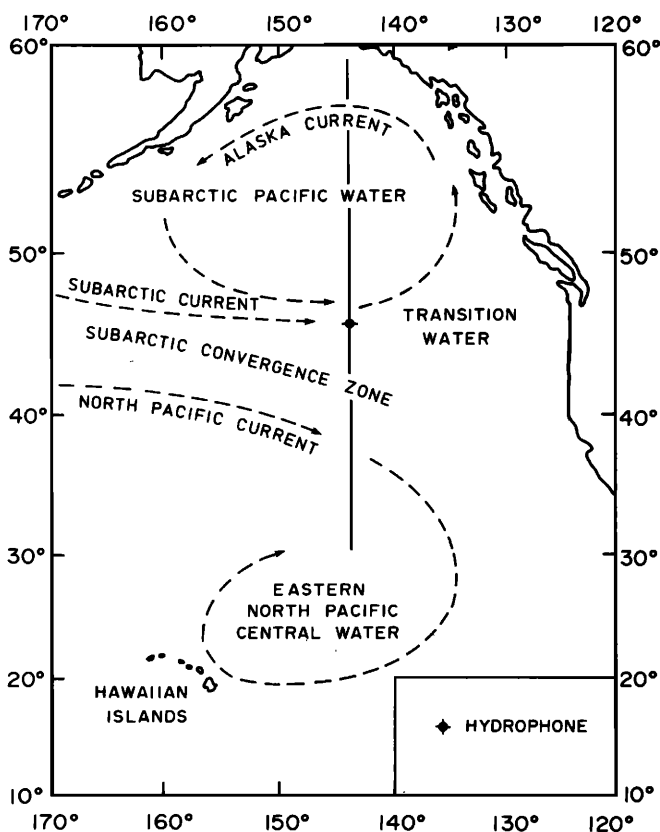


FIG. 1. Region of experiment in Northeast Pacific Ocean. The propagation experiment was conducted along the 143°30'W meridian from 28°N to 55°N with the hydrophone located at 46°N.

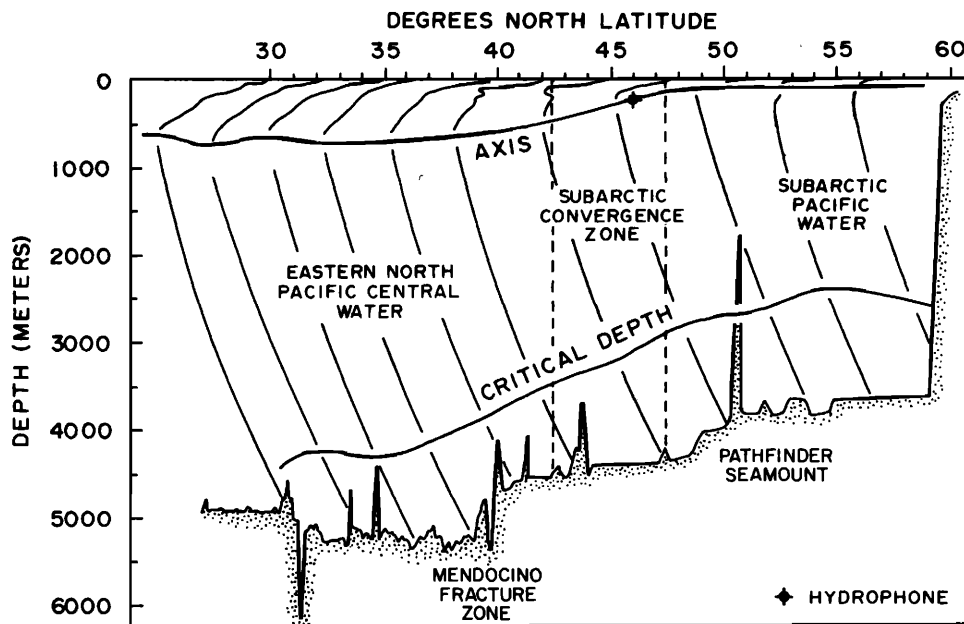


FIG. 2. Bathymetry and sound-velocity profiles along propagation path.

path, the velocity-depth profile shows the deep sound channel axis near 700 m at 40°N rising to 400 m at 46°N. It then rises steeply and begins to merge with the surface sound channel at a depth of about 100 m near 49°N. From about 51°N northward it remains relatively constant at the 100 m depth. There are two notable bathymetric features along the path; the Mendocino Fracture Zone near 40°N and the Pathfinder Seamount near 51°N. To the south of this fracture zone, the average ocean depth increases abruptly by about 600 m to approximately 5300 m and it remains relatively flat southward. North of this zone, the ocean bottom rises gradually from 4700 to 4000 m just south of Pathfinder Seamount. The seamount itself rises to a depth of about 1100 m.

The hydrophone at 46°N was suspended at a depth of 400 m, near the axis of the sound channel at this latitude. The charges were detonated at a depth of 91 m for both the southern and northern runs.

Acoustic signals from each shot were recorded together with a sample of the ambient noise before the shot arrival. For analysis, these time series were segmented, fast-Fourier transformed, and squared. Each of the two resulting energy spectra for the shot plus noise and for the noise alone were integrated over 1/3-octave bands to obtain energies centered at the eight frequencies 25, 50, 100, 160, 250, 400, 630, and 800 Hz. A noise subtraction was carried out to obtain estimates of the received shot energies which, when combined with shot source level values, provided losses in the eight frequency bands.

The accuracy of the propagation loss measurement is dependent on the precision with which the noise removal process can be carried out. This process is in turn dependent on the variability of the noise sample as well as on the signal-to-noise energy ratio (S/N). From an examination of the noise variability, it was estimated that the propagation loss could be measured to within an accuracy of 1 dB provided that only data with a S/N ratio exceeding -3 dB were used in the analysis. The adoption of this criterion had no effect at

low frequencies but it limited the usable data for the two highest frequencies to a maximum range of about 800 km for the southern run.

II. RESULTS

A. Propagation loss

The measured values of the propagation loss in the various 1/3-octave bands are shown in Fig. 3. In the southern run, the convergence zone structure, about 45 km in zone

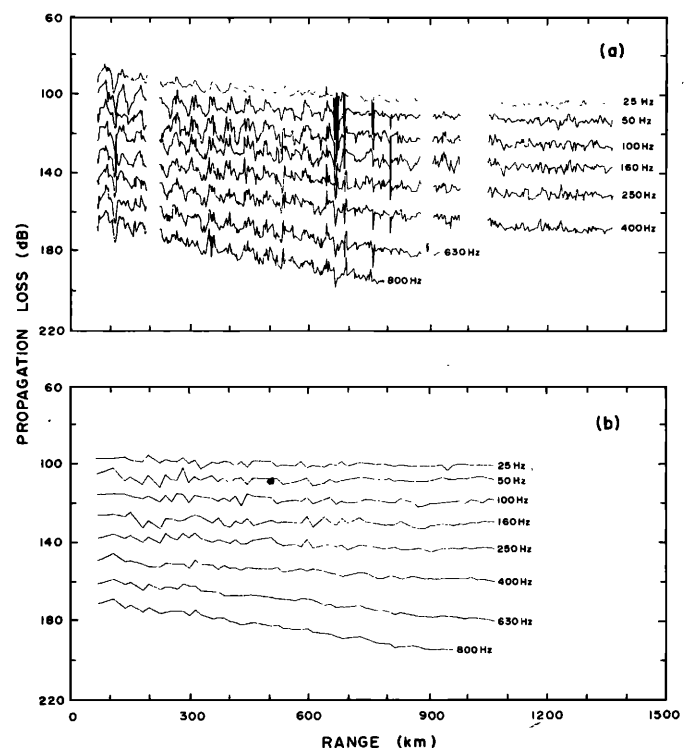


FIG. 3. Propagation loss versus range with successive 10-dB offset starting from 25 Hz. (a) Propagation loss for southern run and (b) northern run.

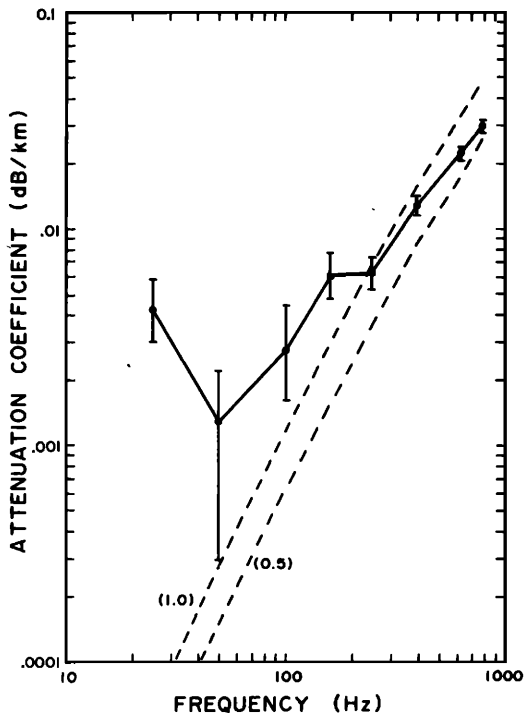


FIG. 4. Attenuation coefficient versus frequency for the southern run. Vertical bars designate the 95% confidence limit. (1.0) denotes Thorp's formula $0.11f^2/(1+f^2) + 0.011f^2$ and (0.5) denotes $0.055f^2/(1+f^2) + 0.011f^2$ (f in kHz).

spacing, is well defined to ranges of several hundred kilometers [Fig. 3(a)]. At high frequencies, the propagation loss increases rapidly with range, in accordance with the steep increase of the attenuation with frequency.

For the northern run [Fig. 3(b)], the propagation loss exhibits considerably different behavior from that observed to the south even allowing for the larger spacing between charge drops. There is greater loss at close ranges and the convergence zones are no longer well defined. Moreover, as the range increases the propagation loss remains relatively constant and, for low frequencies, actually decreases in value. This behavior is attributed to focusing which results from

the shallowing of the deep sound channel to the north.

In both the southern and the northern runs, the propagation loss appears to be unaffected by the bathymetry along the path as neither the Mendocino Fracture Zone nor the Pathfinder Seamount appears to influence the propagation level. This is in agreement with the behavior of long range SOFAR propagation in which most of the acoustic energy is propagated within the deep sound channel.

B. Attenuation coefficient

In the computation of the net volume attenuation, cylindrical spreading is explicitly removed from the measured propagation loss for each frequency band. The residual propagation loss is then fitted by linear regression with the range to yield the net volume attenuation coefficient.

For the southern run, the portion of the data ranging from 38.9°N to 46°N was selected for this computation, where the lower latitude represents the range beyond which the data in the high-frequency bands became unusable. The resultant attenuation coefficient is shown in Fig. 4. Between 250 and 800 Hz, the coefficient lies between the full- (1.0) and half-Thorp (0.5) curves. Below 250 Hz, it begins to deviate from the Thorp curves. It attains a pronounced minimum at 50 Hz with a value of about 0.001 dB/km and then increases to 0.004 dB/km at 25 Hz. The values at 100 and 800 Hz are approximately 0.003 and 0.03 dB/km, respectively. These values are comparable to those determined earlier from the DREP data.⁵

For the northern run, because of the focusing that occurred, similar computation would result in meaningless coefficients; in fact, for frequencies less than 250 Hz, the resulting coefficients would be negative. This focusing can be demonstrated by a computation of the propagation loss via the parabolic equation approximation using experimental velocity-depth profiles and bathymetry along the propagation path. Figure 5 displays the results of such a computation for both the southern and northern runs at 100 Hz. For the southern run, well-defined convergence zones and a steady increase in propagation loss with range repeat the behavior already observed in the corresponding experimental data.

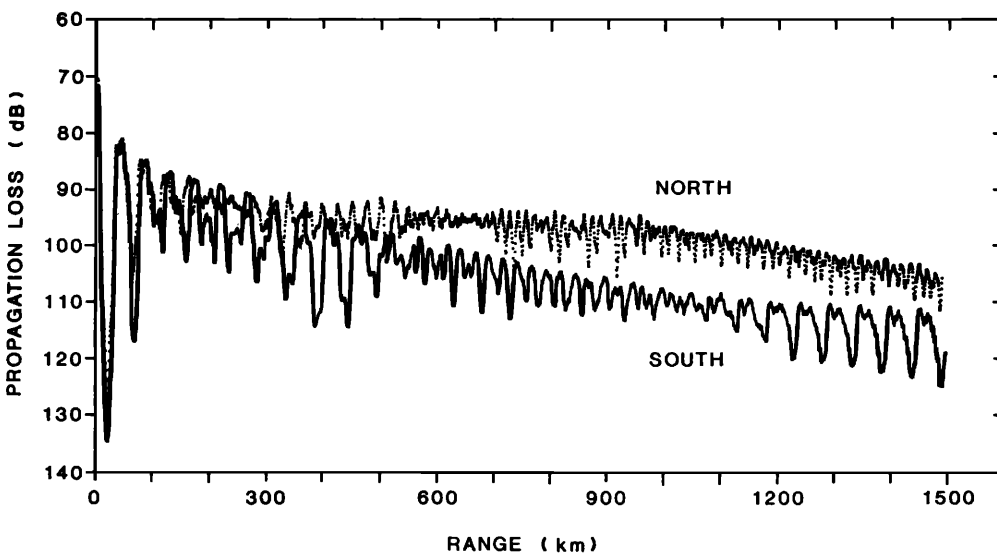


FIG. 5. Comparison of the propagation loss for the northern and southern runs computed at 100 Hz via the parabolic equation approximation. The bathymetry and sound-velocity profiles from Fig. 2 were used.

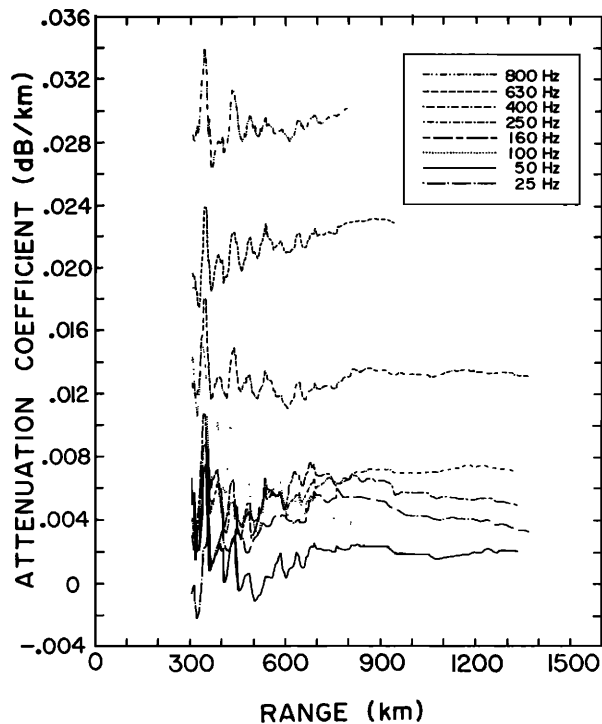


FIG. 6. Variation of the attenuation coefficient with range for the southern run.

However, for the northern run, there is little or no increase in loss with range to about 1000 km and, other than the few zones at close range, there is no convergence zone structure. This also mirrors the behavior of the corresponding experimental data. This atypical behavior is associated with the shallowing of the deep sound channel axis to the north. Due to this shallowing, successive SUS charges detonated closer to the channel axis as the range increased. Thus the propagation became progressively more like axis-to-axis propagation. The consequence of this is twofold: successive shots input a greater portion of the shot energy into the SOFAR propagation and signal enhancement results. Also, in axis-to-axis propagation, convergence zones become less well defined than if either the source or the receiver or both were off the axis.

Recently, Hanna and Rost⁸ pointed out that range-dependent environments could adversely affect the measured attenuation and that no specific form of geometrical spreading assumed can be defensible. The strong signal enhancement in the northern run data and the resultant negative

attenuation coefficient when cylindrical spreading loss is assumed reinforce these authors' conclusion.

C. Spatial variation of the attenuation coefficient

To look for spatial variation in the attenuation coefficient, the propagation loss data for each frequency band in the southern run were divided into sets, each having a common minimum range but with each successive set spanning an increased range interval. For each data set, the attenuation coefficient was computed and plotted against the maximum range of the set. In this manner, the spatial variation of the attenuation coefficient with increasing range can be observed and used as an indication of the range over which a reliable value for the coefficient may be determined.

The spatial variation of the attenuation coefficient is shown in Fig. 6. For each frequency band, the attenuation coefficient undergoes spatial oscillations to a maximum range of approximately 300 to 700 km with a structure somewhat like the convergence zones in the propagation loss data. Beyond 700 km, the oscillations are almost damped out and the coefficients settle to relatively constant values. For greater ranges, there appear to be definite trends with the coefficient increasing and decreasing with range for frequency bands above and below 250 Hz, respectively. However, these variations are within the 95% confidence interval and so their significance is unclear. Note that at ranges in excess of 500 km, the attenuation coefficient at 50 Hz is less than that for all other frequencies which is in keeping with the results displayed in Fig. 4.

¹M. Schulkin and H. W. Marsh, "Sound absorption in sea water," *J. Acoust. Soc. Am.* **34**, 864-865 (1962).

²W. H. Thorp, "Deep ocean sound attenuation in the sub- and low-kilocycle-per-second region," *J. Acoust. Soc. Am.* **38**, 648-654 (1965).

³W. H. Thorp, "Analytical description of the low-frequency attenuation coefficient," *J. Acoust. Soc. Am.* **42**, 270 (1967).

⁴E. Yeager, F. H. Fisher, J. Miceli, and R. Bressel, "Origin of the low-frequency sound absorption in sea water," *J. Acoust. Soc. Am.* **53**, 1705-1707 (1973).

⁵R. H. Mellen and D. G. Browning, "Low-frequency attenuation in the Pacific Ocean," *J. Acoust. Soc. Am.* **59**, 700-702 (1976).

⁶A. C. Kibblewhite, N. R. Bedford, and S. K. Mitchell, "Regional dependence of low-frequency attenuation in the Pacific Ocean," *J. Acoust. Soc. Am.* **61**, 1160-1177 (1977).

⁷A. C. Kibblewhite and L. D. Hampton, "A review of deep ocean sound attenuation data at very low frequencies," *J. Acoust. Soc. Am.* **67**, 147-157 (1980).

⁸J. S. Hanna and P. V. Rost, "The influence of range-dependent environments on low-frequency measurements in the sea," *J. Acoust. Soc. Am.* **61**, 369-374 (1977); see also *J. Acoust. Soc. Am.* **62**, 772 (1977) and **63**, 778 (1977).